Acta Biologica Hungarica 66(1), pp. 66–79 (2015)
DOI: 10.1556/ABiol.66.2015.1.6

LOCALIZATION OF BEN1-LIKE PROTEIN AND NUCLEAR DEGRADATION DURING DEVELOPMENT OF METAPHLOEM SIEVE ELEMENTS IN *TRITICUM AESTIVUM* L.

JINGTONG CAI,[1] ZHIHUI ZHANG,[1] ZHUQING ZHOU,[1]* WENLI YANG,[1] YANG LIU,[1] FANGZHU MEI,[2] GUANGSHENG ZHOU[2] and LIKAI WANG[1]

[1]Laboratory of Cell Biology, College of Life Science and Technology, Huazhong Agricultural University, Wuhan, Hubei 430070, China
[2]College of Plant Sciences & Technology, Huazhong Agricultural University, Wuhan, Hubei 430070, China

(Received: February 28, 2014; accepted: April 28, 2014)

Metaphloem sieve elements (MSEs) in the developing caryopsis of *Triticum aestivum* L. undergo a unique type of programmed cell death (PCD); cell organelles gradually degrade with the MSE differentiation while mature sieve elements keep active. This study focuses on locating BEN1-LIKE protein and nuclear degradation in differentiating MSEs of wheat. Transmission electron microscopy (TEM) showed that nuclei degraded in MSE development. First, the degradation started at 2–3 days after flowering (DAF). The degraded fragments were then swallowed by phagocytic vacuoles at 4 DAF. Finally, nuclei almost completely degraded at 5 DAF. We measured the BEN1-LIKE protein expression in differentiating MSEs. *In situ* hybridization showed that BEN1-LIKE mRNA was a more obvious hybridization signal at 3–4 DAF at the microscopic level. Immuno-electron microscopy further revealed that BEN1-LIKE protein was mainly localized in MSE nuclei. Furthermore, MSE differentiation was tested using a TSQ Zn^{2+} fluorescence probe which showed that the dynamic change of Zn^{2+} accumulation was similar to BEN1-LIKE protein expression. These results suggest that nucleus degradation in wheat MSEs is associated with BEN1-LIKE protein and that the expression of this protein may be regulated by Zn^{2+} accumulation variation.

Keywords: Triticum aestivum L. – MSEs – immuno-electron microcoy – *in-situ* hybridization – BEN1-LIKE protein

INTRODUCTION

Programmed cell death (PCD) is a cell suicide process involving cell condensation, cell shrinkage, and ordered cell disassembly [23]. It was discovered during normal embryological development early in 1951 [10]. Senescence in plant cells was defined as the deteriorative processes which are behind the natural causes of death, which include PCD that first described as present in plants [15]. PCD had been demonstrated to be an active cell death process involved in the development of animals and plants [2, 14], which was accompanied by increased vacuolation, cellular shrinkage,

*Corresponding author; e-mail address: zhouzhuqing@mail.hzau.edu.cn

nuclear condensation, and even DNA fragmentation [9, 17]. In addition, some features of PCD in plants are similar to features characteristic of apoptosis in animals such as the changes in cell morphology and the processing of DNA into oligonucleosome-sized pieces [23].

One of the key similarities between PCD in plant cells and apoptosis in animal cells is the degradation of nuclear DNA [13]. Nuclear endonuclease is essential for DNA fragmentation and other morphologic changes of apoptotic nuclei [13, 22, 27]. In addition, nuclease induction is strongly associated with plant PCD processes [7, 27]. For example, several nucleases have been identified to be responsible for hypersensitive response to cell death signal [18–19]. The isolation and characterization of cDNAs encoding two S1-type DNases (*BEN1* and *ZEN1*) that can be involved in the PCD of plants have been described [1]. Furthermore, Zn^{2+}-dependent endonuclease cDNAs *(Bnuc1)* isolated from salt-stressed or senescent leaves in barley were detected [20]. The S1-type and Zn^{2+}-dependent DNase groups have been associated with PCD [1, 27, 36]. In addition, a previous study revealed an endonuclease which is responsible for DNA laddering by the D-mannose system in *Arabidopsis* roots and maize *(Zea mays)* [26]. The endonuclease genes (*BEN1* and *Bnuc1*) up-regulated in tissues undergoing PCD are expressed during male gametogenesis in barley, and a novel endonuclease gene namely *Bnuc2* has been discovered [36]. In contrast, Domínguez et al. [3, 4] used wheat grain nucellar cells undergoing PCD to analyze nucleus dismantling and identify two endonucleases. However, the endonucleases involved in plant PCD are still largely unknown.

Plant phloem is composed of sieve elements (SEs), companion cells, and phloem parenchyma cells. SEs are responsible for the transport of nutrients, ions, and water [8]. The ultrastructures of the root protophloem SE at different developmental stages of *Arabidopsis thaliana* L. showed chromatin condensation, nuclear degradation and later disappearance, and mitochondria still in the cytoplasm of the mature SEs [33]. In addition, the nuclear control on metabolic processing in the mature SEs was lost, but nuclear remnants of mature SEs still remained in vascular cryptogams and conifers [6, 29]. These studies illustrate that the development of phloem SEs is a PCD process. Nevertheless, the PCD process would discontinue in MSEs and the cells would retain some cytoplasm remnants and keep active [32, 35]. This special PCD in SE differentiation has been named “programmed cell semi-death” [29].

To determine the mechanism of programmed cell semi-death in SEs, we have performed studies to confirm that the cytoplasm degradation is mediated by vacuole microautophagy. Tonoplast then selectively fused with the plasma membrane after vacuole cytoplasm degraded completely. After combing the space a small amount of preserved cytoplasm was discovered [32]. However, the development of SEs involved in PCD is still largely unknown. The wheat endonucleases involved in the SE differentiation of the programmed cell semi-death process are not reported in detail. Without the wheat endonucleases gene sequences, we utilized the endonuclease gene *BEN1* from a higher homology barley plant. This gene was called *BEN1-LIKE*. Using the ventral vascular bundles of caryopses in developing wheat as a model system, we investigated MSE differentiation and nuclear degradation, located the BEN1-LIKE

protein and mRNA, and detected fluorescence of Zn^{2+}. We aimed to determine by TEM and fluorescence microscopy whether these results are associated with SE differentiation of cytological and ultrastructural features.

MATERIALS AND METHODS

Material and sampling

Wheat (*Triticum aestivum* L.) seeds of cv. Huamai 8 were planted in a greenhouse (12 h light/12 h dark, 20 °C) of Huazhong Agricultural University, Hubei Province, China. During the growth of seedlings, they were watered with Hoagland's nutrient solution [11]. At the time of flowering, the flowering spikelets were tagged with a pen mark on the arista and the ears were tagged with labels. Spikelet samples were collected daily from 0 to 7 days after flowering (DAF) for experiment.

Microstructural observation

The microstructure of vascular tissue in caryopses was determined according to Wang's method [31]. Two μm thick sections were cut on an LKB 2088 Ultracut ultramicrotome (Bromma, Sweden). The sections were then stained with 1% (w/v) toluidine blue solution for 5 min at 25 °C and rinsed with ddH_2O. The sections were viewed with a light microscope (Nikon Eclipse 80i, Tokyo, Japan).

Ultrastructural observation

The ultrastructure of the nuclear experiment was determined according to Zhou's method [38]. Then 80–90 nm thick sections were cut on an ultramicrotome and viewed (unstained) with transmission electron microscope (TEM) H-7650 (Hitachi, Japan) at 80 kV.

In situ *hybridization*

All the pre-treatment protocols were adapted from Yang [32]. The paraffin embedded samples were cut on a paraffin slicing machine (Leica RM 2235, Germany) at 5 μm. Oligonucleotides were labeled according to the DIG Oligonucleotide Tailing Kit (Roche, Germany). Immunological detections were performed by alkaline phosphatase-conjugated anti-digoxigenin antibody and visualized with NBT\BCIP (Roche, Germany). The sections were viewed by light microscopy. A positive reaction was indicated by deposition of deep purple.

Oligonucleotides for *BEN1* (Accession No. D83178) (Sangon, China) were as follows: anti-sense oligonucleotide: 5'-gtcga gcagg acgac accct aggag atgag tacta cttca aagcg-3', sense oligonucleotide: 5'-cgctt tgaag tagta ctcat ctcct agggt gtcgt cctgc tcgac-3'.

Immuno electron microscopy of BEN1-LIKE protein

Immuno electron microscopy was carried out according to Liu's method [16]. The 80–90 nm thick sections were cut on an ultramicrotome, incubated with rabbit anti-BEN1-LIKE antibody (Shanghai ImmunoGen Bio-technology, China), stained with 2% uranyl acetate and lead citrate, and examined with a Hitachi H-7650 TEM at 80 kV.

Based on the electron micrographs, we derived numerical statistics regarding the localization of colloidal gold by analyzing more than 40 sieve elements at different stages with the ACDsee PowerPack software (ACD Systems Ltd.). Statistical analysis was carried out via the Excel software (Microsoft Corporation). Data are presented as the mean ± standard deviation. Significant differences were accepted at $P < 0.05$. The control group was exposed to the BSA solution, instead of the first antibody.

Zn^{2+} fluorescence

The Zn^{2+} fluorescence experiment was carried out according to Xu's methods [34]. The sections were cut on a freezing microtome (Leica CM1850, Germany) at 10 μm, stained with TSQ Zn^{2+} fluorescence probe (Enzo) (10 $\mu mol \cdot L^{-1}$), kept for 5 min at 25 °C, and were washed in dd H_2O twice for 5 min. Then sections were viewed using a fluorescence microscope (Nikon Eclipse 80I) under the UV light wavelength (360 ~ 380 nm) excitation. Control group sections were stained with dd H_2O instead of TSQ Zn^{2+} fluorescence probe solution.

RESULTS

Structural changes of developing MSEs of Triticum aestivum *L.*

Microstructures were examined in the developing caryopses of wheat. The cell wall became thicker than the neighboring cells (Fig. 1). We could not find the structure of MSEs at 0 DAF (Fig. 1A), and the MSE cells started growing at 1 DAF (Fig. 1B). As MSEs developed, the number of cells gradually increased. At 6 and 7 DAF, MSEs grow mature which could not be observed in endocyte barely (Fig. 1G–H).

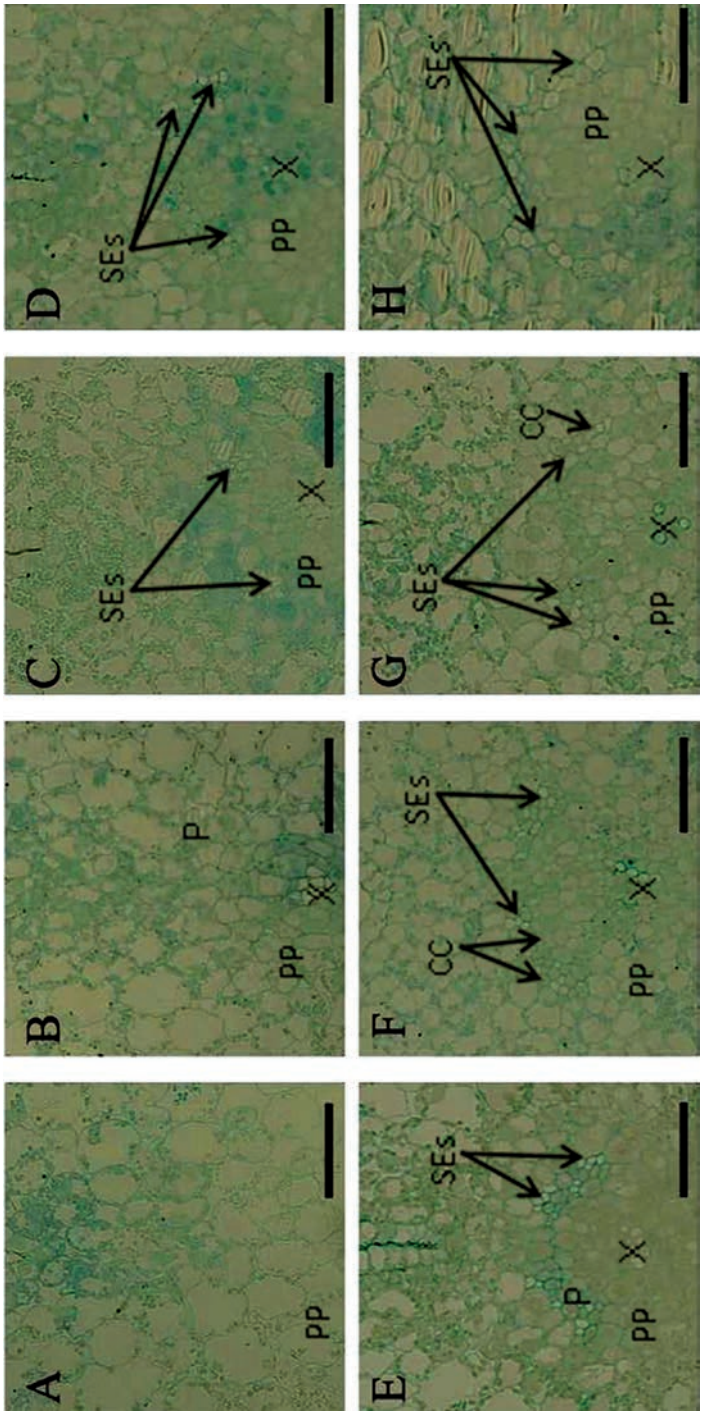

Fig. 1. Structure of the vascular tissue in wheat caryopsis. A, B, C, D, E, F, G, and H are the cross sections at 0–7 DAF respectively. P: phloem; X: xylem; SE: sieve element; CC: companion cells; PP: phloem parenchyma cells. *Bar:* 50 μm

Ultrastructural observation of nuclear degradation in MSEs

At 2 DAF, the nuclei appeared normal and the chromatin condensation could be observed (Fig. 2A, A1) which was similar to that found at 2.5 DAF (Fig. 2B, B1). At 3 DAF, the nuclear invagination appeared, the nuclei were slightly deformed, and the electron density increased due to the aggregation and condensation of chromatin (Fig. 2C, C1). At 3.5 DAF, the nuclei partly degraded and part of the nuclei and cytoplasm were swallowed by vacuoles (Fig. 2D, D1). At a later stage, integral nuclei could not be observed and there was a mass of phagocytic vacuoles which were swallowing the nearby cell content (Fig. 2E, E1). The phagocytic vacuoles were transported to the vacuole that degraded endocytes (Fig. 2F, F1). No nuclei in the MSEs, mitochondria, and amyloplast, which were close to cytomembrane and the membrane fusion, were detected at 5 DAF (Fig. 2G, G1, and G2).

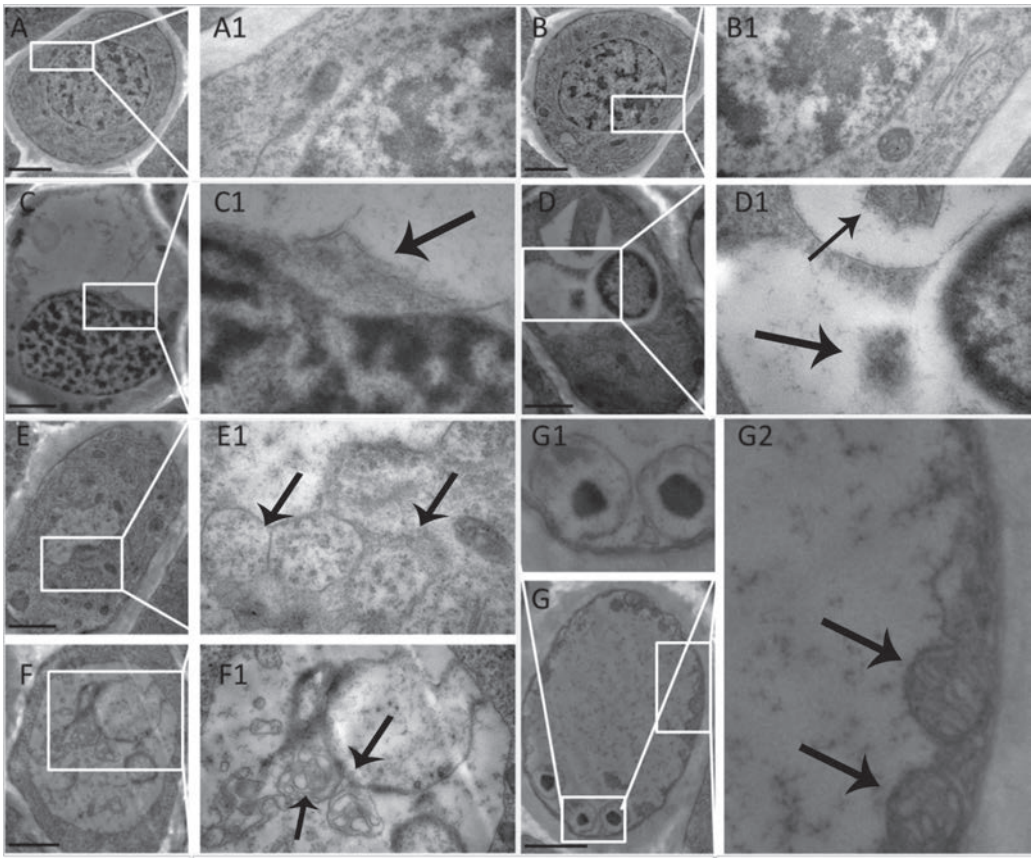

Fig. 2. Changes in the nucleus during the differentiation of MSEs. A: 2 DAF; B: 2.5 DAF; C: 3 DAF; D: 3.5 DAF; E: 4 DAF; F: 4.5 DAF; G: 5 DAF. A1, B1, C1, D1, E1, F1, G1, and G2 are the enlarged areas of the white boxes in A–G, respectively. *Bar:* 2 μm

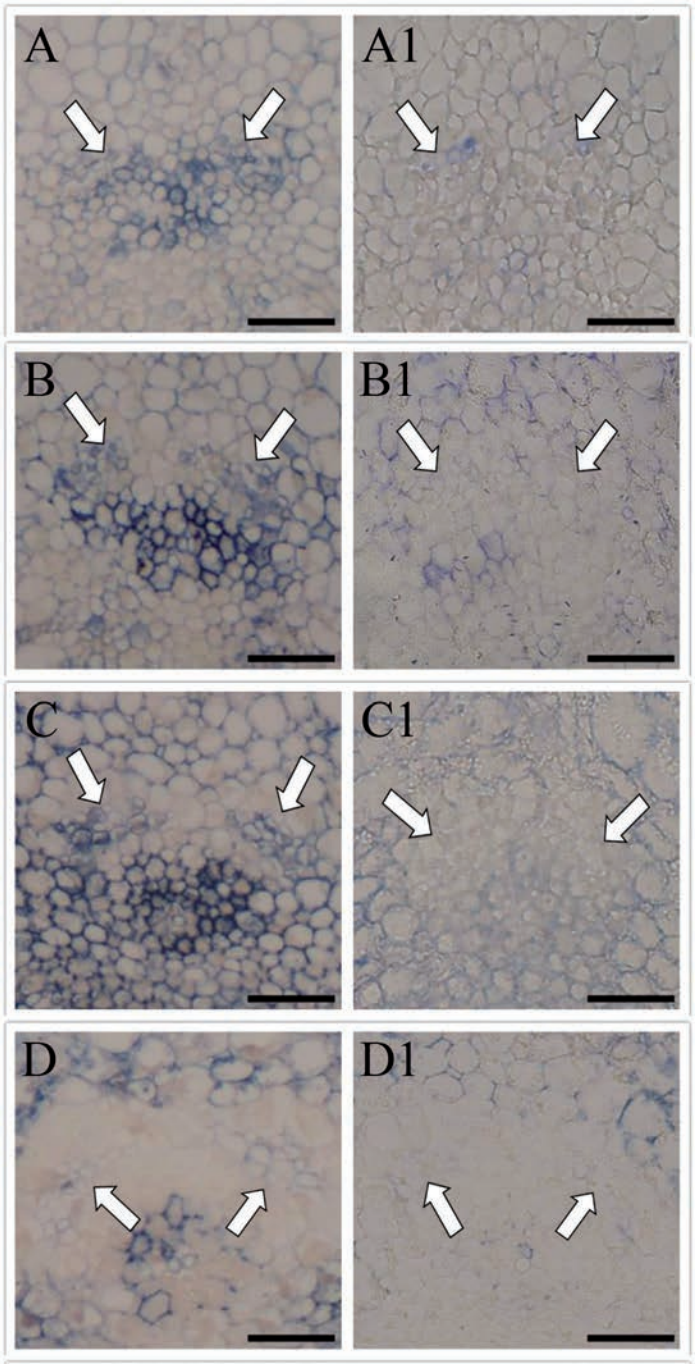
A
A1
B
B1
C
C1
D
D1

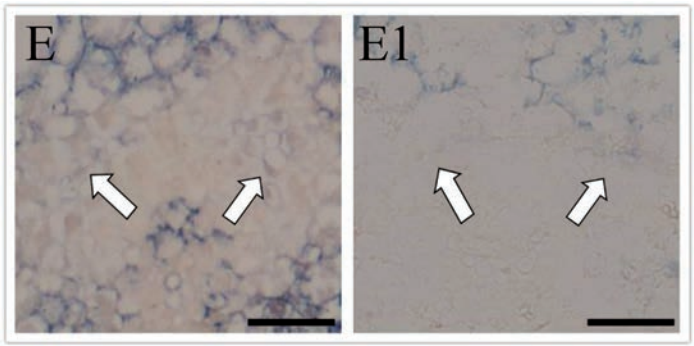

Fig. 3. Localization of *BEN1-LIKE* mRNA in abdominal vascular bundle of caryopses by *in situ* hybridization. A, B, C, D, and E represent the cross section at 2 to 6 DAF, respectively, which were treated with antisense probes. A1, B1, C1, D1, and E1 are control at sense probes. Arrows show the sieve elements. *Bar:* 50 μm

Localization of BEN1-LIKE *mRNA in abdominal vascular bundle of caryopses*

BEN1-LIKE mRNA showed a clear deep purple signal pattern in abdominal vascular tissues of the cross sections of caryopses. The purple positive signal showed mRNA of *BEN1-LIKE* in MSEs, and the signal also remained in the parenchyma cells around MSEs (Fig. 3). The strongest purple signal appeared in MSEs at 3 and 4 DAF (Fig. 3B, C) and gradually decreased at 5 and 6 DAF (Fig. 3D, E). No obvious signals were observed in MSEs of the sense control group (Fig. 3A1–E1).

Immunohistochemical localization of BEN1-LIKE protein in MSEs

Subcellular localization of BEN1-LIKE protein was performed to better elucidate the possible mechanisms involved and its role in MSEs. At early stages of development, young MSEs can be distinguished by cell wall thickness [31]. In this study, BEN1-LIKE protein was localized as black colloidal gold particles (Fig. 4). At 2 DAF, a small number of gold particles that detect BEN1-LIKE protein were observed in cytoplasm and nuclei of sieve elements (Fig. 4A, A1, and A2), but their number did not change obviously (Fig. 5). The labeling intensity was strong at 3 DAF (Fig. 4B, B1, and B2) and was distributed in the nuclei of sieve elements (Fig. 5). At 4 DAF, the gold particles were found in the nucleus fragments and cytoplasm (Fig. 4C, C1, and C2; Fig. 5). At 5 DAF, a small number of gold particles were also detected in the cytoplasm, and cell organelles were almost missing (Fig. 4D, D1, D2; Fig. 5). No labelling appeared in the negative control group (Fig. 4E–H and E1–H1).

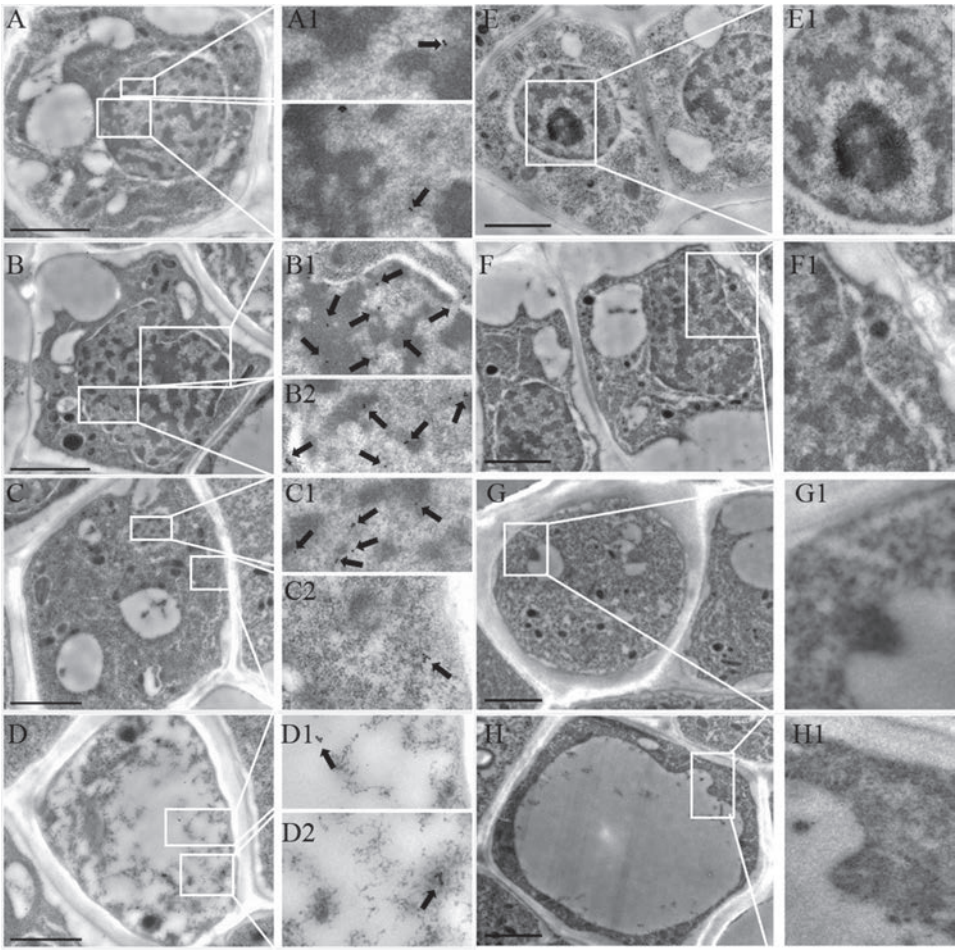

Fig. 4. Subcellular localization of BEN1-LIKE protein by immuno electron microscopy in MSEs of wheat caryopsis. The arrows show the gold particles which represent the BEN1-LIKE protein. A, A1, and A2: 2 DAF. B, B1, and B2: 3 DAF. C, C1, and C2: 4 DAF. D, D1, and D2: 5 DAF. No label appeared in the negative control group at 2 to 5 DAF (E–H, E1–H1). *Bar:* 2 μm

Zn^{2+} fluorescence

To analyze Zn^{2+} briefly, we used a TSQ Zn^{2+}-sensitive fluorescent probe to detect the Zn^{2+} accumulation change in MSE differentiation. The blue fluorescence intensity was brighter at 3 and 4 DAF than at 2 and 5 DAF, and blue autofluorescence in the control group was weak at 4 DAF (Fig. 6). The dynamic Zn^{2+} accumulation changed in a similar pattern as *BEN1-LIKE* expression levels.

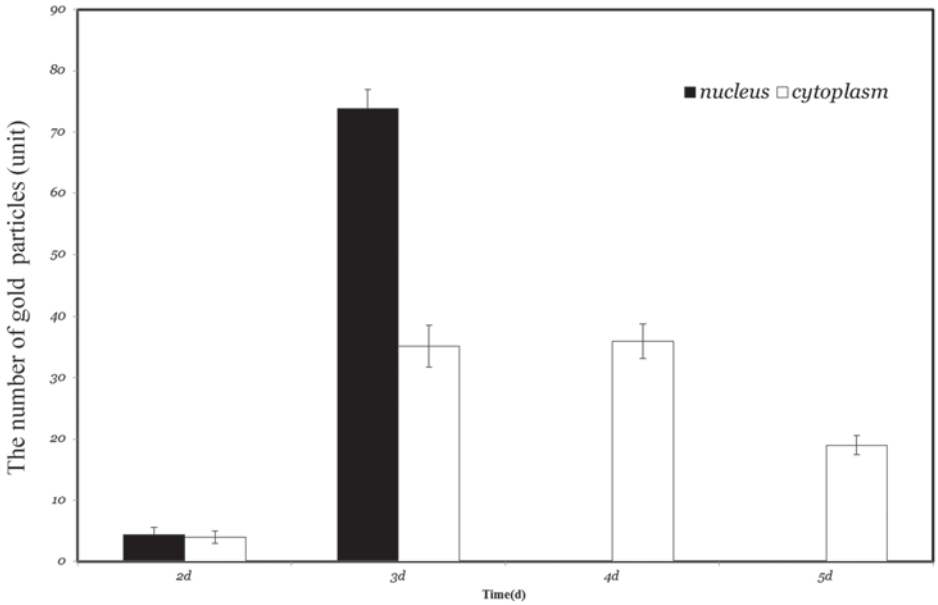

Fig. 5. Distribution of detectable gold particles by immuno electron microscopy in MSEs of wheat caryopsis. Data represent the average value of at least 40 sieve elements. Error bars represent standard deviation

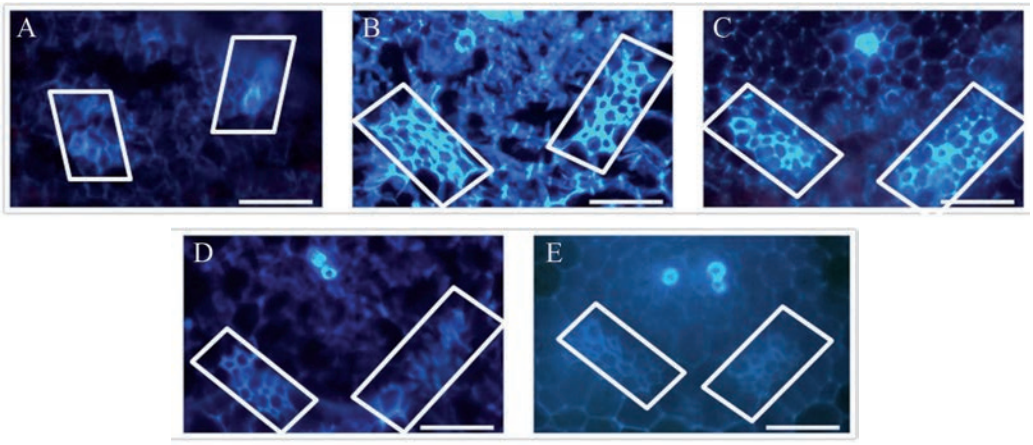

Fig. 6. Zn^{2+} accumulation dynamic change in abdominal vascular bundle of caryopses. A, B, C, and D represent the cross section at 2 to 5 DAF, respectively, which were treated with Zn^{2+}-sensitive fluorescent probe TSQ. The white box shows the sieve elements. E: the control group at 4 DAF. *Bar:* 40 μm

DISCUSSION

Applying TEM and light microscopy, it was found that the MSEs of wheat plants undergo increased vacuolation, cell wall thickening, nuclear degeneration, and chromatin condensation. These characteristics are the same as those reported during the SE differentiation of wheat, *Aegilops comosa* var. *thessalica*, and *Arabidopsis thaliana* L. [5, 33, 35, 37]. They are also typical characteristics of PCD in plants [9, 23]. The mature SEs survived PCD which indicates that PCD in SEs is carefully controlled and the latter cannot be terminated [31]. SEs were previously reported as growing at 0 DAF [35] and maturing at 6 DAF [31]. However, our light microscopic and ultrastructural studies showed that the stage of nucleus degradation was at 3 to 4 DAF (Fig. 2). SEs were found to grow at 1 DAF and most organelles disappeared at 6–7 DAF. It indicates that possibly the growth cycle of MSEs have slight differences.

A typical characteristic of animal apoptosis and plant PCD is nucleus degradation. A case example is the degradation of nuclear chromatin. Chromatin in TEs PCD is degraded by endonuclease which is released from vacuole rupture [21]. Courtois-Moreau et al. [2] pointed out a unique type of cell death program in xylem fibers of hybrid aspen (Populus tremula × P. tremuloides) stems. The degradation of the nuclear and cytoplasmic content occurred before the loss of vacuolar integrity. The vacuoles were thought to initiate cell degradative processes, but the last process occurred before the final autolysis of the remaining cell contents. In addition, vacuole structure was still intact after complete degradation of SE chromatin [32]. Endonucleases in SEs were located in the cytoplasm and nucleus to fulfill its fate of chromatin degradation [32]. Therefore, nuclear chromatin degradation in SEs is inconsistent with TEs. Our ultrastructural observations showed that in the final stage of nucleus degradation at 4 DAF most of the condensed chromatin was lost (Fig. 2) and the remaining condensed chromatin was localized at the periphery of the nucleus [33, 35]. The results showed that nuclear degradation in MSEs mainly happened at 3 to 4 DAF (Fig. 2C, D and E). Condensed chromatin was observed at the edge of nuclei at 3.5 DAF (Fig. 2D, D1), suggesting that fragments of nuclear chromatin were finally degraded by phagocytic vacuoles. The BEN1-LIKE protein, which may be the wheat endonuclease, was also highly expressed at 3–4 DAF (Fig. 4). This suggests that the nucleus degrades in various forms associated with various species-specific genes. Nuclear remnants of SEs at maturity still remained in some plants [6, 29]. Yang [32] has found that fusion to the plasma membrane may preserve a small amount of cytoplasm at the later stage of SEs programmed cell semi-death. We have also found a similar phenomenon in that after the degradation of intact nuclei the nuclear fragments were diffused in the cells and swallowed by the nearby phagocytic vacuoles (Fig. 2E), mitochondria, and amyloplasts which were close to the cytomembrane and membrane fusion. (Fig. 2G, G1, and G2). The result suggests that phagocytic vacuoles possibly play a role in degradation of nuclear fragments by phagocytosis and that a slightly incomplete degradation inclusion may be preserved. This preservation was beneficial to maintaining the activity of SEs and might lead to SEs programmed cell semi-death.

BEN1 is a Zn^{2+}-dependent endonuclease cDNA from barley and has been associated with PCD [1, 27]. Its homology was analyzed with the NCBI Genbank database based on the nucleotide sequences of *BEN1*. The highly homologic sequences are mainly plant endonuclease nucleotide sequences including some predicted genes in wheat. We are not sure whether the highly homologous sequences have the same endonuclease function due to the unknown function of the predicted genes. However, the orthology of wheat and barley was the highest by expressed sequence tag (EST) analysis [33] and *BEN1-LIKE* activity has been shown to be involved in SE development. Thus, we suggest that the BEN1-LIKE protein may be a nuclease that plays a role in differentiation of wheat MSEs. We detected the dynamic change of BEN1-LIKE protein expression in MSEs. Because of the difficulty to specifically extract SEs from caryopsis, we extracted caryopsis abdominal tissue sections by immunochemistry assay to analyze the relative expression of *BEN1-LIKE*. We have found that the higher expression was at 3–4 DAF (Fig. 4) and mainly localized in the nucleus (Fig. 5). Furthermore, *in situ* hybridization indicated that the higher transcription level of *BEN1-LIKE* mRNA was at 3–4 DAF (Fig. 3). We suggest that such a dynamic change of the BEN1-LIKE protein expression in MSEs may be beneficial since it enables the cell to control nuclear degradation.

Wang et al. [31] observed evidence of ceased PCD in MSEs in the developing caryopsis of *Triticum aestivum* L. At maturity, the SEs retain an intact plasmalemma and some organelles, and the mature SEs still act as live cells [32, 35, 37]. It has been shown that Zn^{2+} has a significant impact on apoptosis of plant cells [12–13, 30]. We investigated the dynamic change of Zn^{2+} accumulation in the development of MSEs (Fig. 6) which displayed a similar changing pattern as *BEN1-LIKE* expression levels. *BEN1* is a endonuclease cDNA activated by Zn^{2+} [1, 36], so we suggest that the change of Zn^{2+} accumulation may affect the expression of BEN1-LIKE protein in wheat which is associated with the programmed cell semi-death process in SE differentiation. Two Zn^{2+}-dependent nucleases from intact chloroplasts of leaves of *Oryza sativa* in visible senescence were determined, and when their activity increased markedly the plastid DNA degraded [25]. In addition, DNA ladders were observed during cell death in toxin-treated tomato protoplasts and leaflets, and the intensity of the DNA ladders was inhibited by Zn^{2+} [30]. Moreover, certain levels of Zn^{2+} inhibit the PCD induced by various stresses on the plant cell [30]. Our research indicated that the change of Zn^{2+} accumulation may affect the expression of BEN1-LIKE protein. The high Zn^{2+} accumulation promoted the high *BEN1-LIKE* expression to degrade nuclei at an early stage. The low Zn^{2+} accumulation inhibited the low *BEN1-LIKE* expression at a later stage of MSE differentiation which may have ceased PCD. Due to the difficulty of specifically extracting SEs from caryopsis, Zn^{2+} accumulation precision is limited. Thus, the zinc data are merely correlative. Therefore, we suggest that MSE differentiation in the programmed cell semi-death process may be due to the synergy between BEN1-LIKE protein and Zn^{2+}. The dynamic change of BEN1-LIKE protein and Zn^{2+} is one driver of the programmed cell semi-death phenomenon.

In conclusion, the MSE differentiation may have the following characteristics and causes: 1) The main stage of nucleus degradation is at 3 to 4 DAF. A few incomplete

degradation inclusions may be preserved due to the fusion of phagocytic vacuole membranes and plasma membranes. 2) The higher expression of BEN1-LIKE protein is at 3 and 4 DAF and probably is associated with the MSE programmed cell semi-death differentiation that plays a role in nuclear degradation. 3) The dynamic change in Zn^{2+} accumulation is similar to *BEN1-LIKE* expression levels. The change of Zn^{2+} accumulation may affect the expression of BEN1-LIKE protein and may be associated with the cessation of PCD in MSE differentiation.

ACKNOWLEDGEMENTS

Our deepest gratitude goes first and foremost to the National Nature Science Foundation of China (31071347; 31171469). Moreover, our sincere thanks go to L. Yang who helped us a lot by the study. We also owe our sincere thanks to our family members and friends.

REFERENCES

1. Aoyagi, S., Sugiyama, M., Fukuda, H. (1998) BEN1 and ZEN1 cDNA encoding S1type DNase that associated with programmed cell death in plant. *FEBS Lett. 429,* 134–138.
2. Courtois-Moreau, C. L., Pesquet, E., Sjödin, A., Muniz, L., Bollhöner, B., Kaneda, M., Samuels, L., Jansson, S., Tuominen, H. (2009) A unique program for cell death in xylem fibers of *Populus stem. Plant J. 58,* 260–274.
3. Domínguez, F., Cejudo, F. J. (2006) Identification of a nuclear-localize nuclease from wheat cells undergoing programmed cell death that is able to trigger DNA fragmentation and apoptotic morphology on nuclei from human cells. *Biochem. J. 397,* 529–536.
4. Domínguez, F., Moreno, J., Cejudo, F. J. (2004) A gibberellin-induced nuclease is localized in the nucleus of wheat aleurone cells undergoing programmed cell death. *J. Biol Chem. 279,* 11530–11536.
5. Eleftheriou, E. P., Tsekos, I. (1982) Development of protophloem in roots of *Aegilops comosa* var. *thessalica*, II. Sieve-element differentiation. *Protoplasma 113,* 221–233.
6. Eleftheriou, E. P. (1990) Microtubules and sieve plate development in differentiating protophloem sieve elements of *Triticum aestivum* L. *J. Exp. Bot. 41,* 1507–1515.
7. Farage-Barhom, S., Burd, S., Sonego, L., Perl-Treves, R., Lers, A. (2008) Expression analysis of the BFN1 nuclease gene promoter during senescence, abscission, and programmed cell death-related processes. *J. Exp. Bot. 59,* 3247–3258.
8. Fukuda, H. (2000) Programmed cell death of tracheary elements as a paradigm in plants. *Plant Mol. Biol. 44,* 245–253.
9. Gaffal, K. P., Friedrichs, G. J., El-Gammal, S. (2007) Ultrastructural evidence for a dual function of the phloem and programmed cell death in the floral nectary of Digitalis purpurea. *Ann. Bot. 99,* 593–607.
10. Glücksmann, A. (1951) Cell deaths in normal vertebrate ontogeny. *Biol. Rev. 26,* 59–86.
11. Hoagland, D. R., Snyder, W. C. (1933) Nutrition of strawberry plants under controlled conditions: a) Effects of deficiencies of boron and certain other elements; b) Susceptibility to injury from sodium salts. *Proc. Am. Soc. Hort. Sci. 30,* 288–294.
12. Ito, J., Fukuda, H. (2002) ZEN1 is a key enzyme in the degradation of nuclear DNA during programmed cell death of tracheary elements. *Plant Cell 14,* 3201–3211.
13. Jiang, A. L., Cheng, Y., Li, J., Zhang, W. (2008) A zinc-dependent nuclear endonuclease is responsible for DNA laddering during salt-induced programmed cell death in root tip cells of rice. *J. Plant Physiol. 165,* 1134–1141.
14. Kuriyama, H., Fukuda, H. (2002) Developmental programmed cell death in plants. *Curr. Opin. Plant Biol. 5,* 568–573.

15. Leopold, A. C. (1961) Senescence in plant development: the death of plants or plant parts may be of positive ecological or physiological value. *Science 134,* 1727–1732.
16. Liu, Y., Zhou, Z. Q., Mei, F. Z., Zhou, G. S., Cai, J. T., Yang, W. L., Zhang, Z. H. (2013) Preliminary research on Cathepsin B-like protein in *Triticum aestivum* L. caryopsis and root. *Hubei Agricultural Sciences 52,* 4044–4047.
17. Mea, M. D., Serafini-Fracassini, D., Duca, S. D. (2007) Programmed cell death: similarities and differences in animals and plants: a flower paradigm. *Amino Acids 33,* 395–404.
18. Mittler, R., Lam, E. (1995) Identification, characterization, and purification of a tobacco endonuclease activity induced upon hypersensitive response cell death. *Plant Cell 7,* 1951–1962.
19. Mittler, R., Lam, E. (1997) Characterization of nuclease activities and DNA fragmentation induced upon hypersensitive response cell death and mechanical stress. *Plant Mol. Biol. 34,* 209–221.
20. Muramoto, Y., Watanabe, A., Nakamura, T., Takabe, T. (1999) Enhanced expression of a nuclease gene in leaves of barley plants under salt stress. *Gene 234,* 315–321.
21. Obara, K., Kuriyama, H., Fukuda, H. (2001) Direct evidence of active and rapid nuclear degradation triggered by vacuole rupture during programmed cell death in Zinnia. *Plant Physiol. 125,* 615–626.
22. Peitsch, M. C., Mannherz, H. G., Tschopp, J. (1994) The apoptosis endonucleases: cleaning up after cell death. *Trends Cell Biol. 4,* 37–41.
23. Pennell, R. I., Lamb, C. (1997) Programmed cell death in plants. *Plant Cell 9,* 1157–1168.
24. Shen, R., Liu, X. Y., Zhang, H. X., Zhang, W. (2010) Effect of Zn^{2+} on rice root tip cells programmed cell death under high salt stress or UV-induced. *J. Nanjing Agricult. Univ. 33,* 13–18.
25. Sodmergen, Kawano, S., Tano, S., Kuroiwa, T. (1991) Degradation of chloroplast DNA in second leaves of rice *(Oryza sativa)* before leaf yellowing. *Protoplasma 160,* 89–88.
26. Stein, J. C., Hansen, G. (1999) Mannose induces an endonuclease responsible for DNA laddering in plant cells. *Plant Physiol. 121,* 71–80.
27. Sugiyama, M., Ito, J., Aoyagi, S., Fukuda, H. (2000) Endonucleases. *Plant Mol. Biol. 44,* 387–397.
28. Feng, T. J. (2004) *The Building and Application of Main Crop EST Analysis System.* Dissertation, University of Chinese Academy of Agricultural Sciences, China.
29. van Bel, A. J. E. (2003) The phloem, a miracle of ingenuity. *Plant Cell Environ. 26,* 125–149.
30. Wang, H., Wu, H. M., Cheung, A. Y. (1996) Pollination induces mRNA poly(A) tail-shortening and cell deterioration in flower transmitting tissue. *Plant J. 9,* 715–727.
31. Wang, L. K., Zhou, Z. Q., Song, X. F., Li, J. W., Deng, X. X., Mei, F. Z. (2008) Evidence of ceased programmed cell death in metaphloem sieve elements in the developing caryopsis of *Triticum aestivum* L. *Protoplasma 234,* 87–96.
32. Yang, W. L. (2013) *Study on Programmed Cell Semi-Death of Sieve Elements in Root and Developing Caryopsis of* Triticum aestivum *L.* Dissertation, Huazhong Agricult. Univ., China.
33. Wu, H., Zheng, X. F. (2003) Ultrastructural studies on the sieve elements in root protophleom of *Arabidopsis thaliana. Acta Bot. Sin. 45,* 322–330.
34. Xu, Q. T., Yang, L., Zhou, Z. Q., Mei, F. Z., Qu, L. H., Zhou, G. S. (2013) Process of aerenchyma formation and reactive oxygen species induced by waterlogging in wheat seminal roots. *Planta 238,* 969–982.
35. Yang, C. N., Zhou, Z. Q., Fan, H. Y., Jiang, Z., Mei, F. Z. (2012) Structure-function relationships during metaphloem sieve elements development in *Triticum aestivum*. *Biologia Plantarum 56,* 307–312.
36. Zaina, G., Morassutti, C., De Amicis, F., Fogher, C., Marchetti, S. (2003) Endonuclease genes up-regulated in tissues undergoing programmed cell death are expressed during male gametogenesis in barley. *Gene 315,* 43–50.
37. Zhou, Z. Q., Lan, S. Y., Zhu, X. T., Wang, W. J., Xu, Z. X. (2004) Ultrastructure and its function of phloem cell in abdominal vascular bundle of wheat caryopsis. *Acta Agron. Sin. 30,* 163–168.
38. Zhou, Z. Q., Wang, L. K., Li, J. W., Song, X. F., Yang, C. N. (2009) Study on programmed cell death and dynamic changes of starch accumulation in pericarp cells of *Triticum aestivum* L. *Protoplasma 236,* 49–58.